Structure–Activity Analysis of Semisynthetic Nucleosomes: Mechanistic Insights into the Stimulation of Dot1L by Ubiquitylated Histone H2B

ARTICLE *in* ACS CHEMICAL BIOLOGY · OCTOBER 2009

Impact Factor: 5.33 · DOI: 10.1021/cb9002255 · Source: PubMed

6 AUTHORS, INCLUDING:

Robert Mcginty
Pennsylvania State University
20 PUBLICATIONS **1,422** CITATIONS
SEE PROFILE

Maja Köhn
European Molecular Biology Laboratory
50 PUBLICATIONS **1,508** CITATIONS
SEE PROFILE

Matthew R Pratt
University of Southern California
44 PUBLICATIONS **1,124** CITATIONS
SEE PROFILE

Published in final edited form as:
ACS Chem Biol. 2009 November 20; 4(11): 958–968. doi:10.1021/cb9002255.

Structure activity analysis of semisynthetic nucleosomes: Mechanistic insights into the stimulation of Dot1L by ubiquitylated histone H2B

Robert K. McGinty[†], **Maja Köhn**[‡], **Champak Chatterjee**[†], **Kyle P. Chiang**[†,§], **Matthew R. Pratt**[†,§§], and **Tom W. Muir**[†,*]

[†] Laboratory of Synthetic Protein Chemistry, The Rockefeller University, 1230 York Avenue, New York, NY 10065

[‡] EMBL Heidelberg, Meyerhofstraße 1, 69117, Heidelberg, Germany

Abstract

Post-translational modification of histones plays an integral role in regulation of genomic expression through modulation of chromatin structure and function. Chemical preparations of histones bearing these modifications allows for comprehensive *in vitro* mechanistic investigation into their action to deconvolute observations from genome-wide studies *in vivo*. Previously, we reported the semisynthesis of ubiquitylated histone H2B (uH2B) using two orthogonal expressed protein ligation (EPL) reactions. Semisynthetic uH2B, when incorporated into nucleosomes, directly stimulates methylation of histone H3 lysine 79 (K79) by the methyltransferase, disruptor of telomeric silencing-like (Dot1L). Although recruitment of Dot1L to the nucleosomal surface by uH2B could be excluded, comprehensive mechanistic analysis was precluded by systematic limitations in the ability to generate uH2B in large scale. Here we report a highly optimized synthesis of ubiquitylated H2B bearing a Gly76Ala point mutation (uH2BG76A), yielding tens of milligrams of ubiquitylated protein. uH2BG76A is indistinguishable from the native uH2B by Dot1L, allowing for detailed studies of the resultant trans-histone crosstalk. Kinetic and structure activity relationship analyses using uH2BG76A suggest a non-canonical role for ubiquitin in the enhancement of the chemical step of H3K79 methylation. Furthermore, titration of the level of uH2B within the nucleosome revealed a 1:1 stoichiometry of Dot1L activation.

Histones harbor an extraordinary density of post-translational modifications, including acetylation, methylation, phosphorylation, and ubiquitylation (1,2). Acting directly through enhancement or abbrogation of internucleosomal contacts (3) or indirectly through the recruitment of position-specific binding modules (4), these modifications direct the complex expression of the genome. Monoubiquitylation of H2B on K120 (5) is implicated in diverse nuclear processes, ranging from DNA damage repair and cell-cycle checkpoint regulation, to transcriptional elongation and stimulation of histone lysine methyltransferase activity (6–8). However, the mechanistic role of ubiquitin in these contexts remains elusive. In organisms ranging from yeast to humans, ubiquitylation of H2B is a prerequisite for efficient methylation

*Corresponding Author: Tom W. Muir, The Rockefeller University, 1230 York Avenue, Box 223, New York, NY 10065, p: (212) 327-7368, f: (212) 327-7358, muirt@rockefeller.edu.
[§]Present address: aTyr Pharma, 3565 General Atomics Court, Suite 103, San Diego, CA, 92121
[§§]Present address: Department of Chemistry, University of Southern California, Los Angeles, CA, 90089

Author Contributions: RKM, MK, CC, and KPC prepared new reagents. RKM performed research. RKM, MRP, and TWM designed research. RKM and TWM analyzed data and wrote the paper.

Supporting Information available: This material is free via the Internet.

of H3K79 by Dot1 (9–12). H3K79 methylation maintains transcriptional silencing by demarcating euchromatin-heterochromatin boundaries (13), and much like uH2B, is integral to DNA damage repair pathways (14). Aberations of H3K79 methylation are pathogenic in a subset of mixed lineage leukemia (MLL) fusion leukemias (15). Investigation of the regulation of H3K79 methylation by H2B ubiquitylation is critical to understanding the role of these modifications in normal development and disease states.

In order to elucidate the mechanism of stimulation of Dot1L by uH2B, it is necessary to purify or generate significant quantities of homogenously ubiquitylated H2B. Isolation from lysates is complicated by the coexistence of multiple post-translational modifications of H2B, while *in vitro* reconstitution of the ubiquitin conjugating enzymes leads only to modest yields (9, 16). Moreover, both of these approaches restrict inquiry to native ubiquitin and H2B sequences. Previously, we described the semisynthesis of native uH2B using two orthogonal EPL reactions, ensuring chemical homogeneity and bypassing the cellular ubiquitylation machinery (17). EPL allows for the formation of an amide bond between two polypeptides of recombinant and synthetic origins, one containing a C-terminal thioester, and the other an N-terminal cysteine (18). The absence of cysteines in uH2B necessitates the combination of three polypeptides using two traceless protein ligation strategies: one employing a photolytically removable ligation auxiliary and the other, a chemical desulfurization (Figure 1, panel a and Supplementary Figure 1). We used this semisynthetic uH2B to demonstrate a direct stimulation of Dot1L-mediated intranucleosomal methylation of H3K79 (17). Surprisingly, the stimulatory effect of uH2B is not a result of recruitment of Dot1L to the nucleosomal surface, as Dot1L is able to bind to nucleosomes in the absence of ubiquitylation, suggesting that uH2B may stimulate Dot1L activity through allosteric regulation of Dot1L or the nucleosome itself. At the time, detailed biochemical studies were precluded by limitations in scalability of our semisynthetic strategy. Here we report a highly optimized semisynthesis of uH2B bearing the single G76A point mutation at the C-terminus of ubiquitin, allowing the rapid preparation of tens of milligrams of ubiquitylated protein. Nucleosomes containing uH2BG76A were indistinguishable by Dot1L from those containing uH2B, permitting both a comprehensive kinetic analysis of the role of uH2B in H3K79 methylation and the first structure activity relationship investigation of this complex system.

RESULTS and DISCUSSION

Highly optimized uH2BG76A semisynthesis

We first sought to design a new uH2B semisynthesis, optimizing for efficiency and scalability, while minimizing changes to the native sequence. Central to the inefficiency and low yield of the uH2B semisynthesis is the use of a photolytically removable ligation auxiliary (Figure 1, panel a and Supplementary Figure 1). Firstly, the preparation of the auxiliary requires a complex nine-step solution phase synthesis, ultimately limiting the quantity that can be incorporated into a peptide to be used in EPL (19–21). Furthermore, the auxiliary-mediated ligation reaction requires a minimum of five days to reach 60% completion, owing from the sterically hindered ligation onto a disubstituted amine (17,20). Finally, photolytic removal of the ligation auxiliary, concomitant with the cysteine-protecting group, is poorly scalable and cannot be performed in parallel without multiple irradiation sources. We reasoned that a traditional cysteine-mediated ligation could be substituted for the auxiliary-mediated ligation to attach ubiquitin to an H2B C-terminal peptide, thus alleviating the costly constraints imposed by the ligation auxiliary (Figure 1, panel a, blue). Further replacement of the photolytically removable *S*-(*o*-nitrobenzyl) cysteine protecting group in **1a** with a chemically-labile group would eliminate the need for an irradiation step entirely (Figure 1, panel a, green). Following orthogonal ligation to the N-terminal sequence of H2B, the ligation site cysteines could be

reduced to alanines, leaving a G76A substitution at the C-terminus of ubiquitin as the single sacrifice of the optimized semisynthetic strategy (Figure 1, panel a, yellow).

To this end, peptide **1b** corresponding to residues 117–125 of H2B, bearing an A117C substitution, was synthesized (Supplementary Figure 2). Orthogonal side-chain protection of K120 allowed the selective installment of a cysteine through an isopeptide bond with the ε-NH_2 of K120. This cysteine facilitates ligation to ubiquitin and following desulfurization results in the G76A mutation. Transient protection of the N-terminal cysteine in **1b** as a thiazolidine restricts ubiquitin ligation to the desired site (Figure 1, panel a).

In the first step of the synthesis, an excess of peptide **1b** was ligated to recombinant ubiquitin (1-75)-α-thioester, **2** (Supplementary Figure 3), generated by thiolysis of the corresponding intein fusion protein (Figure 1, panel b, step i). Thioester **2** was quantitatively converted into ubiquitylated peptide **3** within two hours (Supplementary Figure 4). Treatment with methoxylamine *in situ* at pH 5 for 12 h led to complete conversion of the thiazolidine to a cysteine, affording branched protein **4** (Figure 1, panel b, step ii, and Supplementary Figure 4). Notably, purification was unnecessary between the first two synthetic steps, further increasing the overall efficiency of the semisynthetic strategy and limiting losses. Protein **4** was then ligated to an excess of H2B(1-116)-α-thioester, **5** (Supplementary Figure 3), yielding full-length ubiquitylated H2B bearing a cysteine at each of the ligation junctions, **6** (Figure 1, panel b, step iii, and Supplementary Figure 4). Raney nickel (22) or radical-initiated (23) desulfurization smoothly converted both cysteines in **6** to alanines, leaving the native A117 in H2B and a G76A mutation in ubiquitin, thus generating uH2BG76A, **7** (Figure 1, panel b, step iv, and Figure 2, panels a and b).

With this revised semisynthetic route, tens of milligrams of ubiquitylated protein were routinely generated – an increase in excess of ten-fold over our previous methodology. Moreover, by eliminating the sluggish auxiliary-mediated ligation and subsequent purification, the time required to generate ubiquitylated H2B (steps i–iv in Figure 1, panel b) was halved. Eliminating the need for photolytic removal of protecting groups not only further enhanced the scalability of the semisynthesis, but also negated the need for specialized optics. Most importantly, all materials required for the solid phase synthesis of peptide **1b** are commercially available, obviating time intensive solution phase organic synthesis and significantly increasing the accessibility of this methodology.

uH2BG76A is indistinguishable from uH2B

We envisioned that a G76A mutation in ubiquitin would be tolerated by any biochemical processes that recognize elements of ubiquitin and its target protein without specifically engaging the isopeptide bond between them (24). In these cases, the ubiquitylated protein with the G76A mutation would likely be indistinguishable from the native protein. Conversely, we reasoned that processes recognizing the isopeptide bond directly might be disrupted by the mutation. Indeed, the ubiquitin G76A mutant is efficiently mobilized and transferred to target proteins *in vivo*, but the conjugated product is resistant to many deubiquitylating enzymes (DUBs) (25,26). Surprisingly, uH2BG76A was recognized and deubiquitylated by ubiquitin C-terminal hydrolase L3 (UCH-L3), to a similar extent as the native control (Figure 2, panel c). Cleaved ubiquitin and ubiquitin G76A were identified by liquid chromatography-mass spectrometry, verifying hydrolysis of the isopeptide bond (Supplementary Figure 5). Furthermore, recognition of uH2B by a linkage-specific anti-uH2B antibody was only slightly decreased by introduction of the G76A mutation (Figure 2, panel d). Key to our goals was the effect of the uH2BG76A mutation on the stimulation of Dot1L. In order to test this, uH2B (17) and uH2BG76A were reconstituted into nucleosomes with recombinant histone proteins (Supplementary Figure 6) and 147 bp of the 601 positioning sequence (27) and submitted to radioactive methyltransferase assays with full-length Dot1L, isolated from an insect cell over

expression system. uH2BG76A stimulated methyltransferase acitivity to levels comparable to uH2B (Figure 2, panel e), validating this mutant as an equally acceptable surrogate for the native sequence in biochemical analysis.

Kinetic analysis of Dot1L stimulation

Disruption of H2B ubiquitylation in organisms from yeast to humans decreases levels of higher order methylation of H3K79 without altering levels of monomethylation (10,28). However, *in vitro* ubiquitylation of H2B drastically increases the level of Dot1L-mediated monomethylation and dimethylation in nucleosomes (17). This pattern is observed with full-length Dot1L as well as the catalytic domain alone. We predicted that analysis of steady-state kinetics would provide insight into the effect of uH2B on the ability of Dot1L to perform the initial methylation of H3K79. Accordingly, the catalytic domain of Dot1L, containing the first 416 residues of the methyltransferase, was isolated following overexpression in *Escherichia coli* as a GST fusion protein ($Dot1L_{cat}$). Nucleosomes containing H2B or uH2BG76A were prepared with the 146 bp α-satellite palindromic sequence (29). Initial rates of nucleosome methylation by $Dot1L_{cat}$ were obtained by measuring transfer of a radioactive methyl group from *S*-adenosyl methionine, illustrating a vast rate enhancement due to ubiquitylation (Figure 3, panel a). At early time points, only monomethylation of H3K79 was detected, allowing for the direct steady-state velocity analysis of the first methylation event (Figure 3, panel b). Under steady-state conditions (Figure 3, panel c), $Dot1L_{cat}$ clearly followed Michaelis-Menten kinetics in the monomethylation of ubiquitylated nucleosomes (K_m of 3.3 ± 0.6 μM and a k_{cat} of 1.16 ± 0.09 s^{-1}). However, under all reasonable conditions tested, $Dot1L_{cat}$ failed to show any concentration dependence toward unmodified nucleosomes. This could result from an exorbitantly high K_m or an immeasurably low k_{cat}. The latter could reflect an extremely slow chemical step and/or a decreased rate of product release. To probe this further, we performed $Dot1L_{cat}$ methyltransferase reactions under single turnover-type conditions (Figure 3, panel d). Even at saturating levels, $Dot1L_{cat}$ was far more efficient in methylation of ubiquitylated nucleosomes, suggesting an increase in the velocity of the chemical step of the first methylation. While these experiments do not prevent dimethylation, early time points are likely restricted to a single methylation, mimicking a single turnover paradigm. This suggests a conformational change in the active site complex of Dot1L bound to H3K79.

The calculated K_m for Dot1L-mediated monomethylation of ubiquitylated nucleosomes is similar to values calculated for other histone lysine methyltransferases acting on peptide and protein substrates (30–35); however, the k_{cat} of Dot1L on ubiquitylated nucleosomes is 10 to 100 times greater than reported values for these other reactions, suggesting a rate enhancement on nucleosomal substrates. Similar to yeast Dot1 (36), Dot1L appears to be distributive enzyme, as evidenced by its ability to monomethylate an excess of substrate without measurable accumulation of dimethylation (Figure 3, panel b). Although a direct comparison of kinetic parameters of Dot1L on ubiquitylated and unmodified nucleosomes was not possible, it is clear that Dot1L is able to monomethylate uH2B bearing nucleosomes to a much greater extent than unmodified nucleosomes. This seems contradictory to *in vivo* experiments where levels of H3K79 monomethylation are apparently unaffected by genetic disruption of H2B ubiquitylation (10,28). We propose that accumulation over time or parallel pathways may compensate specifically for any deficit in monomethylation of K79 in the absence of H2B ubiquitylation *in vivo*.

Structure activity analysis of uH2B nucleosomes

A myriad of small chemical modifications to histones, such as acetylation, phosphorylation, and methylation, have evolved to control accessibility of genomic loci and to tune the recruitment and activity of effectors of genomic expression (1,4). Given these established mechanisms, why would nature select such a large modification in ubiquitin, when a smaller

modification might suffice? To delve into this question, we performed a structure activity relationship analysis of the role of ubiquitin in Dot1L stimulation.

We first wondered whether the ubiquitin fold was essential to stimulate methyltransferase activity. Could the mere acylation of H2BK120 be sufficient? We synthesized a truncated uH2B (tr-uH2B) lacking the globular domain of ubiquitin (Figure 4, panels a and b). First, peptide **1c** was synthesized corresponding to residues 117–125 of H2BA117C, with residues 72–76 of ubiquitin attached to the ε-NH_2 of K120 (Supplementary Figure 7). Similar to peptide **1b**, orthogonal protection of K120 allowed the C-terminal residues of ubiquitin to be installed through an isopeptide bond with K120. The N-terminus of the ubiquitin branch was acetylated to prevent interference during EPL. Ligation of **1c** to H2B(1-116)-α-thioester, **5**, followed by Raney nickel-mediated desulfurization afforded tr-uH2B (Supplementary Figure 8). Nucleosomes assembled with 147 bp of 601 sequence containing tr-uH2B were assayed against full-length Dot1L. However, the presence of tr-uH2B did not lead to an increase in methyltransferase activity over that observed for unmodified nucleosomes (Figure 4, panel d), suggesting that the ubiquitin fold is necessary for Dot1L stimulation.

We next asked whether a specific surface of ubiquitin was required, or whether a protein of similar size and shape could substitute. We replaced ubiquitin with Smt3, the yeast homolog of human Small Ubiquitin-like Modifier 1 (SUMO1) (Figure 4, panel a). Smt3 has a similar overall fold to that of ubiquitin (Figure 4, panel c), but only a 17% sequence identity (37). An HA-Smt3(2-97)-α-thioester (Supplementary Figure 3) was substituted for the ubiquitin thioester, **2**, in the semisynthetic strategy. Steps xv-xvii proceeded smoothly (Supplementary Figure 8), but no protein was recovered after incubation with Raney nickel. Therefore, the pre-desulfurization product, sH2B(cys), bearing an A117C mutation in H2B and a G98C mutation in Smt3, was incorporated into nucleosomes. Unlike nucleosomes containing the non-desulfurized uH2B(cys), **6**, sH2B(cys) nucleosomes failed to stimulate Dot1L to significant levels (Figure 4, panel d). This result suggests that a surface of ubiquitin is recognized specifically.

We turned our attention to the interaction of ubiquitin with ubiquitin binding proteins. In almost all cases reported, ubiquitin interactions involve a hydrophobic patch including leucine 8 (L8) and isoleucine 44 (I44) (Figure 3, panel b) (24). Mutation of one or both residues to alanine typically abrogates binding (38–40). We generated mut-uH2B containing the triple alanine mutant L8A/I44A/G76A by replacing thioester **2**, with the corresponding thioester bearing the L8A/I44A double mutation (Supplementary Figure 3) and proceeding with the two EPL reactions and desulfurization (Figure 3, panel a and Supplementary Figure 8). Dot1L was able to methylate nucleosomes bearing mut-uH2B to a similar degree as those bearing uH2BG76A (Figure 4, panel e). Therefore, a non-canonical interaction surface of ubiquitin seems to be involved in stimulation of Dot1L, likely by binding to the nucleosome, Dot1L, or both. This raises the possibility that multiple surfaces of ubiquitin are interpreted simultaneously by parallel pathways, thereby, necessitating the recognition of non-canonical surfaces. This could explain the evolutionary need for such a large modification. Further investigation of the role of the surfaces of uH2B in H3K79 methylation and its myriad of other downstream processes will put this hypothesis to the test.

If ubiquitin binds Dot1L leading to allosteric activation, ubiquitin added in *trans* might be able to increase methylation of unmodified nucleosomes. However, at 1 mM exogenous ubiquitin, no stimulation of Dot1L was observed (Supplementary Figure 9). In contrast, if ubiquitin binds to the nucleosome, mutations on the nucleosomal surface surrounding the site of ubiquitin attachment might prevent stimulation of Dot1L activity by decoupling ubiquitylation with changes to the nucleosomal structure. Previously, alanine scanning of the yeast nucleosome revealed two mutants in the acidic patch of H2A that prevent H3K4 methylation, which is also

directly stimulated by uH2B (16), without an observable effect on ubiquitylation of H2B (41). We reasoned that if H3K4 methylation is coupled to uH2B through a similar mechanism as H3K79 methylation, these mutations might disrupt Dot1L stimulation in our system. We prepared nucleosomes containing unmodified H2B or uH2BG76A in combination with each of the mutations, H2AE64A and H2AN68A (Figure 5, panel a and Supplementary Figure 6). Neither mutation altered Dot1L stimulation by uH2B (Figure 5, panel b), indicating divergent roles for uH2B in methylation of H3K4 and K79.

The basic patch of H4 is critical to the action of yeast Dot1 in telomeric silencing (42). Simultaneous mutation of two arginines in H4 at positions 17 and 19 to alanines (R17/19A) nearly abolishes H3K79 methylation in yeast (43). We wondered if the same pattern would hold true for human Dot1L and if ubiquitylation could overcome any deficit in methylation due to the mutations. Nucleosomes were prepared containing H4R17/19A (Figure 5 and Supplementary Figure 6) and either unmodified H2B or uH2BG76A. The H4R17/19A mutation decreased Dot1L activity on unmodified nucleosomes (Figure 5, panel c). A similar decrease was observed with nucleosomes containing uH2BG76A (Figure 5, panel b). Therefore, while conserved from yeast to humans, mutation of the basic patch seems to disrupt Dot1 activity independent of ubiquitylation.

One uH2B stimulates methylation of one H3K79

To date, Dot1L activity has only been studied in the context of homogenously ubiquitylated nucleosomes, where each copy of H2B is ubiquitylated. Given a 1% prevalence of uH2B *in vivo* (5), statistically, it is likely that heterogeneously ubiquitylated nucleosomes are predominant. This raises the question: can a nucleosome bearing one ubiquitylated H2B stimulate Dot1L? If so, will the methyltransferase activity be confined to one copy of H3, or is one uH2B sufficient to drive methylation of H3 on both sides of the nucleosome? To address these questions, we reconstituted histone octamers, varying the ratio of H2B to uH2BG76A. Electrophoretic analysis of the purified octamers confirmed incorporation of appropriate levels of unmodified and ubiquitylated H2B (Figure 6, panel a). Separation of nucleosomes formed with each octamer sample by native gel electrophoresis verified independent assortment of the two forms of H2B, with singly ubiquitylated nucleosomes exhibiting an intermediate electrophoretic mobility when compared to doubly ubiquitylated and unmodified nucleosomes (Figure 6, panel b). Methyltransferase assays showed a linear relationship between the level of uH2BG76A in a nucleosome and the activity of Dot1L, suggesting that one ubiquitylation stimulates methylation of only one H3K79 (Figure 6, panels b and c). However, whether uH2B stimulates methylation of the same nucleosomal surface or the opposite surface cannot be determined from this set of experiments. As further validation of this result, a pool of nucleosomes reconstituted from octamers containing an equal mixture of unmodified and ubiquitylated H2B, have two singly ubiquitylated nucleosomes for every one doubly ubiquitylated nucleosome; yet, half of the methyltransferase activity observed by fluorography occurred on the doubly ubiquitylated nucleosomes.

Conclusion

In summary, we have developed a robust, scalable semisynthesis of ubiquitylated proteins to overcome shortcomings of our previously reported strategy (17). This methodology allowed us to perform detailed kinetic and structure activity relationship analyses of the stimulation of Dot1L-mediated methylation of H3K79 by ubiquitylated H2B. These studies suggest that a non-canonical interaction surface of the ubiquitin fold leads to activation of the chemical step of Dot1L-mediated H3K79 monomethylation. Moreover, titration of the level of uH2B within a nucleosome allowed the demonstration of a 1:1 stimulation of H3K79 methylation by ubiquitylation. As both modifications are integral to regulation of expression and maintenance

of integrity of the genome (44), a full illumination of their mechanisms is key to understanding their roles in development and disease.

This greatly improved semisynthetic strategy will also allow the facile and rapid preparation of other ubiquitylated histones, and more broadly, other ubiquitylated proteins. This is especially important in systems where the natural abundance of ubiquitylated proteins is low or where ubiquitin conjugating enzymes are unknown or unavailable. Additionally, as we have illustrated here, chemical control of both ubiquitin and the target protein permits detailed analysis of the mechanisms underlying signaling through monoubiquitylation.

METHODS

Peptide synthesis

Peptide **1a** was synthesized as previously described (17). For peptide **1b**, the sequence corresponding to residues 117–125 of *Xenopus* H2B with an A117C substitution was synthesized on pre-loaded Wang resin using automatic solid-phase peptide synthesis with a 9-fluorenylmethoxycarbonyl (Fmoc) N^{α} protection strategy and using 2-(1H-benzotriazole-1-yl)-1,1,3,3-tetramethyluronium hexafluorophosphate (HBTU) for amino acid activation. Standard ^{t}butyl side-chain protection was used throughout with the following exceptions; the ε-amino group of K120 was protected with the 4-methyltrityl (Mtt) group, and the thiol group of C117 was installed as an N^{α}-(^{t}butoxycarbonyl)-thiazolidine (Boc-thiazolidine). The Mtt group on K120 was deprotected by successive incubations of the peptidyl-resin with 1% TFA in DCM containing 1% triisopropylsilane (TIS) for 10 min intervals, until no yellow color evolved. Boc-*S*-trityl-cysteine was coupled to the ε-NH_2 of K120. Following cleavage from the resin with TFA:TIS:H_2O (95:2.5:2.5) for 3 h, peptide **1b** was purified by RP-HPLC on a process scale using a 6–18% B gradient over 60 min (A: 0.1% trifluoroacetic acid (TFA) in water; B: 90% acetronitrile, 0.1% TFA in water), yielding 56 mg peptide from 0.25 mmol resin. Peptide **1b** was characterized by ESI-MS [$(M+H)^+$ observed: 1,115.9 Da; expected: 1,115.3 Da].

Expressed protein ligation reaction 1

The ligation reaction between peptide, **1b**, and ubiquitin(1-75)-MES, **2**, was performed using conditions similar to those previously optimized for the corresponding auxiliary-mediated reaction (17). In a typical reaction, purified peptide **1b**, (19.9 mg, 17.9 μmol) and protein **2** (45.7 mg, 5.3 μmol) were combined in 2.5 mL of ligation buffer (6 M guanidinium chloride, 300 mM sodium phosphate, 100 mM MESNa, 50 mM tris(2-carboxyethyl)phosphine (TCEP), pH 7.8). The pH was adjusted to 7.8 using 5 N NaOH and the reaction was allowed to proceed for 4 h at room temperature. After 2 h, reaction completion was verified by RP-HPLC and ESI-MS. [$(M+H)^+$ observed = 9,609 ± 2 Da; $(M+H)^+$ expected = 9,606 Da]

Cysteine deprotection

To crude ligation product **3** was added 2.5 mL 50% HPLC buffer B and 0.72 mL 4 M methoxylamine, to reach a final concentration of 0.5 M. The pH of the resulting solution was increased to 5 with 5 N NaOH. Following incubation for 12 h at room temperature to allow complete deprotection of the cysteine, product, **4**, was purified by preparative RP-HPLC using a 25–55% B gradient over 45 min, yielding 27.3 mg purified protein. The identity of the purified protein **4** was verified by ESI-MS. [$(M+H)^+$ observed = 9,593 ± 2 Da; $(M+H)^+$ expected = 9,594 Da]

Expressed Protein Ligation reaction 2

In a typical reaction, protein **4** (29.9 mg, 3.1 μmol), and H2B(1-116)-MES, **5** (52.6 mg, 4.0 μmol), were dissolved in ligation buffer to a final volume of 1.6 mL. The pH of the resulting solution was increased to 7.8 with 5 N NaOH and the reaction was allowed to proceed for 48 h. Fresh TCEP was then added to a final concentration of 50 mM. The ligation product, **6**, was purified using semi-preparative RP-HPLC with a 35–52% B gradient over 45 min, yielding 38.4 mg of protein **6**. The identity of the ligation product was verified by ESI-MS. [$(M+H)^+$ observed = 22,444 ± 5 Da; $(M+H)^+$ expected = 22,443 Da]

Desulfurization

The 38.4 mg of protein **6** was converted to 30 mg uH2BG76A, **7**, using using two complementary desulfurization methodologies. Raney nickel reduction was used to convert C117 and C76 of protein **6** to alanines (17,22,45). In a typical reaction, protein **6**, (8.0 mg, 0.36 μmol) was dissolved in 3 mL desulfurization buffer 1 (6 M guanidinium chloride, 200 mM sodium phosphate, 35 mM TCEP, pH 7.0). Raney nickel was prepared as previously described (17) and added at 0 h, 6.5 h, 10 h, and 13.5 h. The reaction progress was followed by RP-HPLC and ESI-MS. After 22 h, the Raney nickel was pelleted by centrifugation and washed. The reaction supernatant and washes were combined, added to an equivalent volume of 50% HPLC buffer B, and purified using semi-preparative RP-HPLC with a 42–52% B gradient over 45 min, yielding 4.0 mg of uH2BG76A, **7**. Protein **7** was characterized by ESI-MS.

Protein **6** was also desulfurized by the previously reported radical-initiated methodology (23, 46). In a typical reaction, protein **6**, (9.0 mg, 0.40 μmol) was dissolved in 500 μL desulfurization buffer 2 (6 M guanidinium chloride, 200 mM sodium phosphate, pH 7.0). To this solution was added 10 μl ethane thiol, 750 μl 0.5 M TCEP (dissolved in desulfurization buffer followed by pH adjustment to 7.0), 50 μl 2-methylpropane thiol, and 12.5 μl 0.2 M VA-061 (Wako Chemicals) (dissolved in methanol), and the mixture was incubated in a 37 °C water bath. The reaction progress was followed by RP-HPLC and ESI-MS. After 24 h, the product was purified using semi-preparative RP-HPLC with a 42–52% B gradient over 45 min, yielding 7.6 mg of uH2BG76A, **7**. Protein **7** was characterized by ESI-MS. [$(M+H)^+$ observed = 22,380 ± 4 Da; $(M+H)^+$ expected = 22,379 Da]

Methyltransferase assays

Full-length Dot1L and $Dot1L_{cat}$ were prepared as previously described (17). Methyltransferase assays with Dot1L were performed as previously described (17). Ubiquitin (Sigma) was added as indicated. Methyltransferase assays for steady-state measurements were performed as follows: Serial two-fold dilutions of nucleosomes from 7.5 μM to 230 nM were preformed in methyltransferase assay buffer (20 mM Tris HCl, 4 mM EDTA, 1 mM DTT, pH 7.9) supplemented with 1.6 μM ^{3}H SAM at 4 °C. Each solution was aliquoted into individual PCR tubes. The reaction was initiated by the addition of $Dot1L_{cat}$ (2 nM, 4 nM, and 6 nM) and subsequent transfer to a 30 °C water bath. For nucleosomes containing uH2BG76A, 5 μL assay samples were quenched at 3 min by the addition of 10 μL 0.2 % TFA and spotted on filter paper for liquid scintillation counting as previously described (17). For unmodified nucleosomes, 10 μL assay samples were quenched at 15 min and quantified as above. Each concentration of nucleosome was assayed against each concentration of $Dot1L_{cat}$ in duplicate. Counts from reactions containing no $Dot1L_{cat}$ were subtracted from each sample. Conversion of CPM to moles of methylation was performed using LC-MS with isoptopically-labelled synthetic standards. Unmodified and monomethylated peptides containing residues 73–83 of H3 and a d_5 isotopically-labelled Phe78 (Fmoc-Phe(d5)-OH from Cambridge Isotopes) were added into gel slices containing assay samples. Propionylation, trypsin digestion, and propionylation were performed as previously described (47). Relative quantities were determined by standardizing spectral counts of modified tryptic peptides to synthetic

isotopically-labelled peptides following LC-MS/MS using a Dionex U3000 capillary/nano-HPLC system (Dionex) directly interfaced with the Thermo-Fisher LTQ-Orbitrap mass spectrometer (Thermo Fisher). In a typical experiment, a conversion factor (*F*) of $2.15*10^{-16}$ mol/CPM was calculated. Values of v_o/E_T were calculated using equation (1),

$$\frac{v_0}{E_T} = \frac{F(\mathrm{CPM}_{obs} - \mathrm{CPM}_{background})}{t * E_T} \quad (1)$$

where v_o is the initial velocity, E_T is the molar quantity of $Dot1L_{cat}$ in the volume quantified, and *t* is time in seconds. Kinetic parameters for the methylation of ubiquitylated nucleosomes were obtained by fitting to the non-linear Michaelis-Menten equation (2) using profit 6.1.1 with the Levenberg-Marquardt algorithm:

$$\frac{v_0}{E_T} = \frac{k_{cat}[S]}{K_m + [S]} \quad (2)$$

where [S] is the concentration of nucleosome. Time courses were fit to linear regression models to verify steady-state conditions.

Assays performed with an excess of $Dot1L_{cat}$ were set up as follows: Nucleosome and $Dot1L_{cat}$ were combined in methyltransferase assay buffer supplemented with 1 μM ^{3}H SAM and 4 μM cold SAM, at 250 nM and 5 μM concentrations, respectively. The reaction was initiated by transferring to a 30 °C water bath. Samples were removed, quenched, and counted as described above. The observed CPM value at 0 sec was subtracted from the observed CPM value after 15, 30, 60, 120, 300, 600, and 6,000 sec. The corrected value was multiplied by 5 to account for dilution with cold SAM and divided by the number of microliters quantified. The appropriate conversion factor (*F*) was applied to calculate methyltransferase activity at each time point. The resultant curves were fit to a single exponential model (3) using profit 6.1.1.

$$\mathrm{Activity} = ae^{-bt} + c \quad (3)$$

For mass spectrometric analysis of methylation levels, assays were submitted to trypsin digestion as previously described (17). Tryptic peptides were analyzed by LC-MS as described above.

Asymmetrically ubiquitylated nucleosomes

Octamers were prepared as described previously described (17) using mixtures of uH2BG76A and H2B. Incorporation of the appropriate levels of ubiquitylated and unmodified H2B was verified by separation on a Criterion 15% Tris HCl gel, followed by Coomassie staining. Nucleosomes were reconstituted on a small scale as previously described (17) and analyzed on a Criterion 5% TBE gel. Each nucleosome sample was subjected to methyltransferase assays as described above. Results, relative to homogenously ubiquitylated nucleosomes, were compared to theoretical values for each model tested, assuming negligible methylation of unmodified nuclesomes. If each uH2BG76A stimulates methylation of one H3K79 within the nucleosome, the simple linear model (4) is expected.

$$\text{Rel.CPM}=f_{ub} \quad (4)$$

where f_{ub} is fraction of H2B that is ubiquitylated. Assuming independent assortment of uH2BG76A and H2B, if each uH2BG76A stimulates methylation of both H3K79 within the nucleosome, the non-linear model (5) is expected.

$$\text{Rel.CPM}=f_{ub}^2+2(f_{ub})(1-f_{ub}) \quad (5)$$

which simplifies to equation (6).

$$\text{Rel.CPM}=-f_{ub}^2+2f_{ub} \quad (6)$$

Supplementary Material

Refer to Web version on PubMed Central for supplementary material.

Acknowledgments

We would like to acknowledge H Deng and H Yu at The Rockefeller University Proteomics Resource Center for mass spectrometric analysis of methylated peptides and hydrolyzed ubiquitin. We would like to thank J Kim for assistance in preparing Dot1L and S Darst and S Feng for assistance with the Model 491 Prep cell. We would like to thank D Allis, R Roeder, and O Andersen for many stimulating discussions. This work was funded by the U. S. National Institutes of Health and the Starr Cancer Consortium. RKM was supported by NIH MSTP grant GM07739. MRP and KPC were supported by the American Cancer Society.

References

1. Kouzarides T. Chromatin modifications and their function. Cell 2007;128:693–705. [PubMed: 17320507]
2. Wang Z, Zang C, Rosenfeld JA, Schones DE, Barski A, Cuddapah S, Cui K, Roh TY, Peng W, Zhang MQ, Zhao K. Combinatorial patterns of histone acetylations and methylations in the human genome. Nat Genet 2008;40:897–903. [PubMed: 18552846]
3. Shogren-Knaak M, Ishii H, Sun JM, Pazin MJ, Davie JR, Peterson CL. Histone H4-K16 acetylation controls chromatin structure and protein interactions. Science 2006;311:844–7. [PubMed: 16469925]
4. Taverna SD, Li H, Ruthenburg AJ, Allis CD, Patel DJ. How chromatin-binding modules interpret histone modifications: lessons from professional pocket pickers. Nat Struct Mol Biol 2007;14:1025–40. [PubMed: 17984965]
5. West MH, Bonner WM. Histone 2B can be modified by the attachment of ubiquitin. Nucleic Acids Res 1980;8:4671–80. [PubMed: 6255427]
6. Game JC, Chernikova SB. The role of RAD6 in recombinational repair, checkpoints and meiosis via histone modification. DNA Repair (Amst) 2009;8:470–82. [PubMed: 19230796]
7. Weake VM, Workman JL. Histone ubiquitination: triggering gene activity. Mol Cell 2008;29:653–63. [PubMed: 18374642]
8. Giannattasio M, Lazzaro F, Plevani P, Muzi-Falconi M. The DNA damage checkpoint response requires histone H2B ubiquitination by Rad6-Bre1 and H3 methylation by Dot1. J Biol Chem 2005;280:9879–86. [PubMed: 15632126]
9. Zhu B, Zheng Y, Pham AD, Mandal SS, Erdjument-Bromage H, Tempst P, Reinberg D. Monoubiquitination of human histone H2B: the factors involved and their roles in HOX gene regulation. Mol Cell 2005;20:601–11. [PubMed: 16307923]

10. Kim J, Hake SB, Roeder RG. The human homolog of yeast BRE1 functions as a transcriptional coactivator through direct activator interactions. Mol Cell 2005;20:759–70. [PubMed: 16337599]
11. Ng HH, Xu RM, Zhang Y, Struhl K. Ubiquitination of histone H2B by Rad6 is required for efficient Dot1-mediated methylation of histone H3 lysine 79. J Biol Chem 2002;277:34655–7. [PubMed: 12167634]
12. Briggs SD, Xiao T, Sun ZW, Caldwell JA, Shabanowitz J, Hunt DF, Allis CD, Strahl BD. Gene silencing: trans-histone regulatory pathway in chromatin. Nature 2002;418:498. [PubMed: 12152067]
13. Singer MS, Kahana A, Wolf AJ, Meisinger LL, Peterson SE, Goggin C, Mahowald M, Gottschling DE. Identification of high-copy disruptors of telomeric silencing in Saccharomyces cerevisiae. Genetics 1998;150:613–32. [PubMed: 9755194]
14. Bostelman LJ, Keller AM, Albrecht AM, Arat A, Thompson JS. Methylation of histone H3 lysine-79 by Dot1p plays multiple roles in the response to UV damage in Saccharomyces cerevisiae. DNA Repair (Amst) 2007;6:383–95. [PubMed: 17267293]
15. Krivtsov AV, Feng Z, Lemieux ME, Faber J, Vempati S, Sinha AU, Xia X, Jesneck J, Bracken AP, Silverman LB, Kutok JL, Kung AL, Armstrong SA. H3K79 methylation profiles define murine and human MLL-AF4 leukemias. Cancer Cell 2008;14:355–68. [PubMed: 18977325]
16. Kim J, Guermah M, McGinty RK, Lee JS, Tang Z, Milne TA, Shilatifard A, Muir TW, Roeder RG. RAD6-Mediated transcription-coupled H2B ubiquitylation directly stimulates H3K4 methylation in human cells. Cell 2009;137:459–71. [PubMed: 19410543]
17. McGinty RK, Kim J, Chatterjee C, Roeder RG, Muir TW. Chemically ubiquitylated histone H2B stimulates hDot1L-mediated intranucleosomal methylation. Nature 2008;453:812–6. [PubMed: 18449190]
18. Flavell RR, Muir TW. Expressed protein ligation (EPL) in the study of signal transduction, ion conduction, and chromatin biology. Acc Chem Res 2009;42:107–16. [PubMed: 18939858]
19. Pellois JP, Muir TW. A ligation and photorelease strategy for the temporal and spatial control of protein function in living cells. Angew Chem Int Ed Engl 2005;44:5713–7. [PubMed: 16059958]
20. Chatterjee C, McGinty RK, Pellois JP, Muir TW. Auxiliary-mediated site-specific peptide ubiquitylation. Angew Chem Int Ed Engl 2007;46:2814–8. [PubMed: 17366504]
21. Marinzi C, Offer J, Longhi R, Dawson PE. An o-nitrobenzyl scaffold for peptide ligation: synthesis and applications. Bioorg Med Chem 2004;12:2749–57. [PubMed: 15110856]
22. Yan LZ, Dawson PE. Synthesis of peptides and proteins without cysteine residues by native chemical ligation combined with desulfurization. J Am Chem Soc 2001;123:526–33. [PubMed: 11456564]
23. Wan Q, Danishefsky SJ. Free-radical-based, specific desulfurization of cysteine: a powerful advance in the synthesis of polypeptides and glycopolypeptides. Angew Chem Int Ed Engl 2007;46:9248–52. [PubMed: 18046687]
24. Hurley JH, Lee S, Prag G. Ubiquitin-binding domains. Biochem J 2006;399:361–72. [PubMed: 17034365]
25. Pickart CM, Kasperek EM, Beal R, Kim A. Substrate properties of site-specific mutant ubiquitin protein (G76A) reveal unexpected mechanistic features of ubiquitin-activating enzyme (E1). J Biol Chem 1994;269:7115–23. [PubMed: 8125920]
26. Hodgins RR, Ellison KS, Ellison MJ. Expression of a ubiquitin derivative that conjugates to protein irreversibly produces phenotypes consistent with a ubiquitin deficiency. J Biol Chem 1992;267:8807–12. [PubMed: 1315740]
27. Lowary PT, Widom J. New DNA sequence rules for high affinity binding to histone octamer and sequence-directed nucleosome positioning. J Mol Biol 1998;276:19–42. [PubMed: 9514715]
28. Shahbazian MD, Zhang K, Grunstein M. Histone H2B ubiquitylation controls processive methylation but not monomethylation by Dot1 and Set1. Mol Cell 2005;19:271–7. [PubMed: 16039595]
29. Luger K, Mader AW, Richmond RK, Sargent DF, Richmond TJ. Crystal structure of the nucleosome core particle at 2.8 A resolution. Nature 1997;389:251–60. [PubMed: 9305837]
30. Collazo E, Couture JF, Bulfer S, Trievel RC. A coupled fluorescent assay for histone methyltransferases. Anal Biochem 2005;342:86–92. [PubMed: 15958184]

31. Dirk LM, Flynn EM, Dietzel K, Couture JF, Trievel RC, Houtz RL. Kinetic manifestation of processivity during multiple methylations catalyzed by SET domain protein methyltransferases. Biochemistry 2007;46:3905–15. [PubMed: 17338551]
32. Trievel RC, Beach BM, Dirk LM, Houtz RL, Hurley JH. Structure and catalytic mechanism of a SET domain protein methyltransferase. Cell 2002;111:91–103. [PubMed: 12372303]
33. Patnaik D, Chin HG, Esteve PO, Benner J, Jacobsen SE, Pradhan S. Substrate specificity and kinetic mechanism of mammalian G9a histone H3 methyltransferase. J Biol Chem 2004;279:53248–58. [PubMed: 15485804]
34. Chin HG, Patnaik D, Esteve PO, Jacobsen SE, Pradhan S. Catalytic properties and kinetic mechanism of human recombinant Lys-9 histone H3 methyltransferase SUV39H1: participation of the chromodomain in enzymatic catalysis. Biochemistry 2006;45:3272–84. [PubMed: 16519522]
35. Eskeland R, Czermin B, Boeke J, Bonaldi T, Regula JT, Imhof A. The N-terminus of Drosophila SU (VAR)3-9 mediates dimerization and regulates its methyltransferase activity. Biochemistry 2004;43:3740–9. [PubMed: 15035645]
36. Frederiks F, Tzouros M, Oudgenoeg G, van Welsem T, Fornerod M, Krijgsveld J, van Leeuwen F. Nonprocessive methylation by Dot1 leads to functional redundancy of histone H3K79 methylation states. Nat Struct Mol Biol 2008;15:550–7. [PubMed: 18511943]
37. Mossessova E, Lima CD. Ulp1-SUMO crystal structure and genetic analysis reveal conserved interactions and a regulatory element essential for cell growth in yeast. Mol Cell 2000;5:865–76. [PubMed: 10882122]
38. Beal R, Deveraux Q, Xia G, Rechsteiner M, Pickart C. Surface hydrophobic residues of multiubiquitin chains essential for proteolytic targeting. Proc Natl Acad Sci U S A 1996;93:861–6. [PubMed: 8570649]
39. Kang RS, Daniels CM, Francis SA, Shih SC, Salerno WJ, Hicke L, Radhakrishnan I. Solution structure of a CUE-ubiquitin complex reveals a conserved mode of ubiquitin binding. Cell 2003;113:621–30. [PubMed: 12787503]
40. Shih SC, Katzmann DJ, Schnell JD, Sutanto M, Emr SD, Hicke L. Epsins and Vps27p/Hrs contain ubiquitin-binding domains that function in receptor endocytosis. Nat Cell Biol 2002;4:389–93. [PubMed: 11988742]
41. Nakanishi S, Sanderson BW, Delventhal KM, Bradford WD, Staehling-Hampton K, Shilatifard A. A comprehensive library of histone mutants identifies nucleosomal residues required for H3K4 methylation. Nat Struct Mol Biol 2008;15:881–8. [PubMed: 18622391]
42. Altaf M, Utley RT, Lacoste N, Tan S, Briggs SD, Cote J. Interplay of chromatin modifiers on a short basic patch of histone H4 tail defines the boundary of telomeric heterochromatin. Mol Cell 2007;28:1002–14. [PubMed: 18158898]
43. Fingerman IM, Li HC, Briggs SD. A charge-based interaction between histone H4 and Dot1 is required for H3K79 methylation and telomere silencing: identification of a new trans-histone pathway. Genes Dev 2007;21:2018–29. [PubMed: 17675446]
44. Wood A, Schneider J, Shilatifard A. Cross-talking histones: implications for the regulation of gene expression and DNA repair. Biochem Cell Biol 2005;83:460–7. [PubMed: 16094449]
45. Pentelute BL, Kent SB. Selective desulfurization of cysteine in the presence of Cys(Acm) in polypeptides obtained by native chemical ligation. Org Lett 2007;9:687–90. [PubMed: 17286375]
46. Chiang KP, Jensen MS, McGinty RK, Muir TW. A Semisynthetic Strategy to Generate Phosphorylated and Acetylated Histone H2B. Chembiochem. 2009
47. Garcia BA, Hake SB, Diaz RL, Kauer M, Morris SA, Recht J, Shabanowitz J, Mishra N, Strahl BD, Allis CD, Hunt DF. Organismal differences in post-translational modifications in histones H3 and H4. J Biol Chem 2007;282:7641–55. [PubMed: 17194708]
48. Vijay-Kumar S, Bugg CE, Cook WJ. Structure of ubiquitin refined at 1.8 A resolution. J Mol Biol 1987;194:531–44. [PubMed: 3041007]
49. Davey CA, Sargent DF, Luger K, Maeder AW, Richmond TJ. Solvent mediated interactions in the structure of the nucleosome core particle at 1.9 a resolution. J Mol Biol 2002;319:1097–113. [PubMed: 12079350]

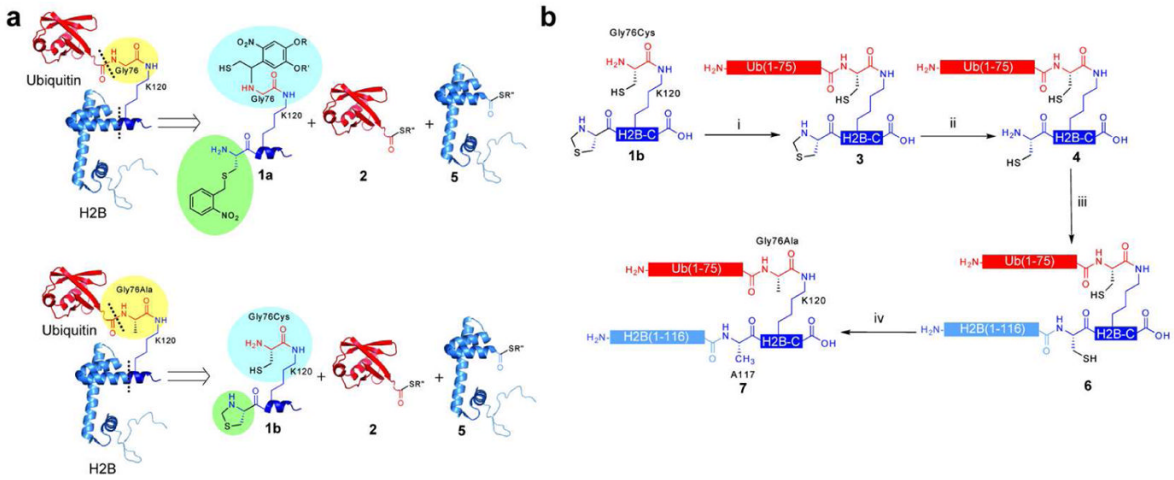

Figure 1. Semisynthesis of uH2BG76A

a, Retrosynthetic comparison of uH2B (top) and uH2BG76A (bottom) syntheses. Both were generated via a 3-piece ligation strategy with the following polypeptides: synthetic peptide containing residues 117–125 of H2B and bearing an A117C mutation, H2B-C, **1a** and **1b**; recombinant ubiquitin(1-75)-α-thioester **2**; and recombinant H2B(1-116)-α-thioester **5**. For the semisynthesis of uH2BG76A, the ligation auxiliary was replaced with a cysteine (blue) and the photolytically removable cysteine protecting group was replaced with a thiazolidine (green). The resultant ubiquitylated proteins differ only at position 76 of ubiquitin (yellow). Dashed lines indicate junctions formed by EPL reactions. **b,** Synthetic scheme for the generation of uH2BG76A. i) EPL was used to ligate peptide **1b** to protein **2**, forming branched protein **3**. ii) Ligation product **3** was treated with methoxylamine at pH 5, affording **4**. iii) Ligation of protein **4** to protein **5**, forming uH2BA117C/G76A, **6**. iv) Raney nickel or radical-initiated desulfurization of protein **6**, forming uH2BG76A, **7**. R = $CH_2CH_2CH_2C(O)NHCH_3$; R′ = CH_3; R″ = $CH_2CH_2SO_3H$.

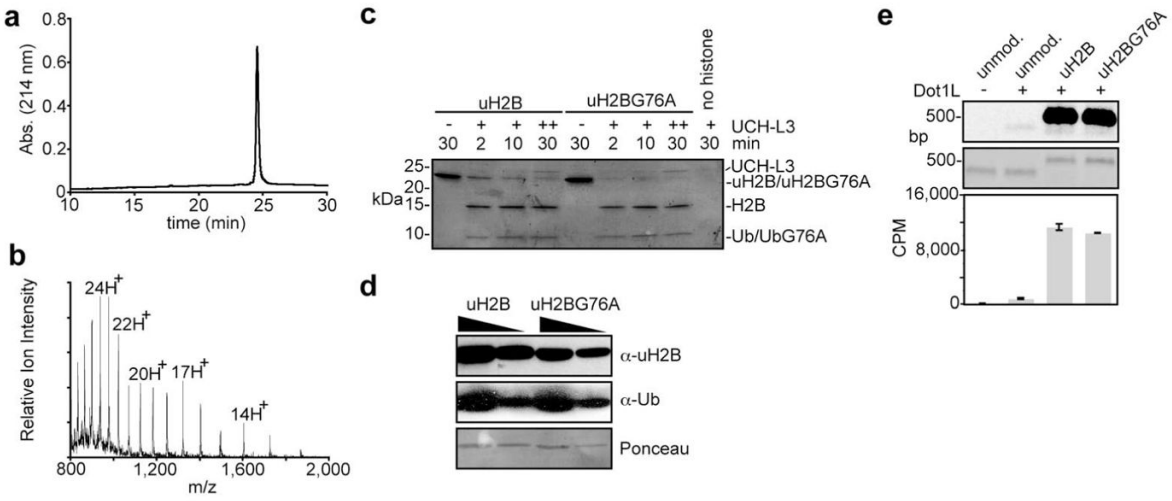

Figure 2. Validation of uH2BG76A as a surrogate for uH2B

a, Reversed phase high performance liquid chromatography (RP-HPLC) chromatogram of purified uH2BG76A, **7. b,** Electrospray ionization mass spectrometry (ESI-MS) spectrum of purified uH2BG76A, **7**. Charge states are labelled. [$(M+H)^+$ observed = 22,380 ± 4 Da (s.d.). $(M+H)^+$ expected = 22,379 Da.] **c,** UCH-L3-mediated hydrolysis of uH2B and uH2BG76A. Coomassie stained gel of assay samples quenched after indicated times. + indicates addition of UCH-L3 at 0 min; ++ indicates addition of UCH-L3 at 0 and 10 min. **d,** Western blot of uH2B and uH2BG76A with linkage specific α-uH2B antibody (top panel). Western blot with α-ubiquitin antibody (middle panel) and ponceau stain (bottom panel) represent loading controls. **e,** Dot1L methyltransferase assay on uH2B and uH2BG76A containing nucleosomes. Nucleosomes methylated with ^{3}H *S*-adenosyl methionine (SAM) were separated on native gels and stained with ethidium bromide (middle panel) prior to probing for ^{3}H methyl incorporation by fluorography (top panel). Quantification of methyltransferase activity was performed by filter-binding followed by liquid scintillation counting (bottom panel). Error bars represent one s.d. (n = 3).

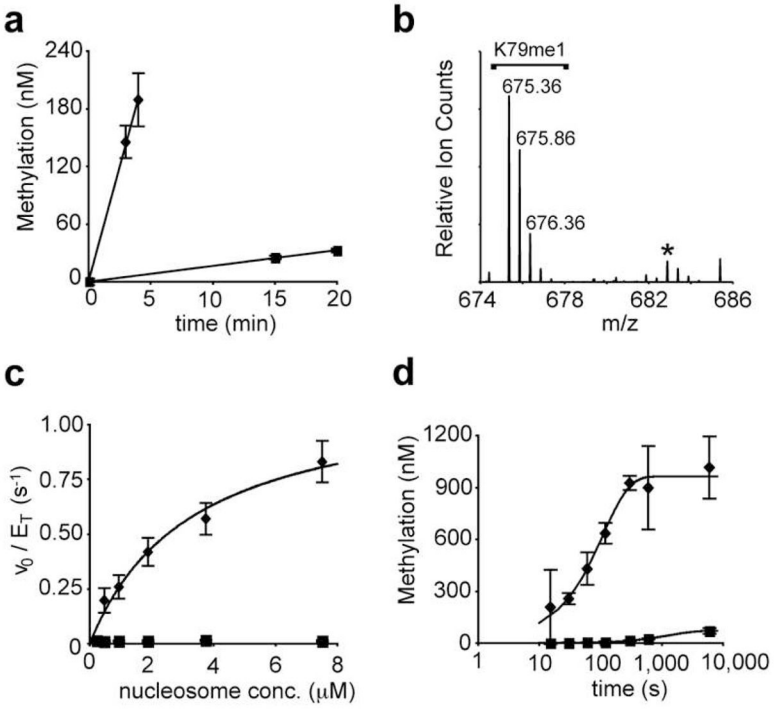

Figure 3. Kinetic analysis of Dot1L-mediated methylation of uH2BG76A nucleosomes

a, Representative time course of $Dot1L_{cat}$-mediated methylation of 0.9 μM nucleosome bearing H2B (squares) or uH2BG76A (diamonds). Linear regression models of the data are shown. Error bars represent one s. d. (n = 2). **b,** LC-MS/MS chromatogram showing K79 monomethylation (K79me1) in the absence of dimethylation for uH2BG76A nucleosomes at 1.8 μM. $[M+2H]^{2+}$ charge states are labelled. An asterisk marks a contaminant that is not dimethylated K79. **c,** Steady-state kinetic analysis of $Dot1L_{cat}$ activity of nucleosomes bearing H2B (squares) or uH2BG76A (diamonds). Fit of uH2BG76A data to the Michaelis-Menten model is shown. Error bars represent one s. d. (n = 6). **d,** Kinetic analysis of methylation of nucleosomes bearing H2B (squares) or uH2BG76A (diamonds) by excess $Dot1L_{cat}$. X-axis is shown in $\log_{10}$ scale to emphasize early time points. Single exponential modelling of the data is shown. Error bars represent one s. d. (n = 3).

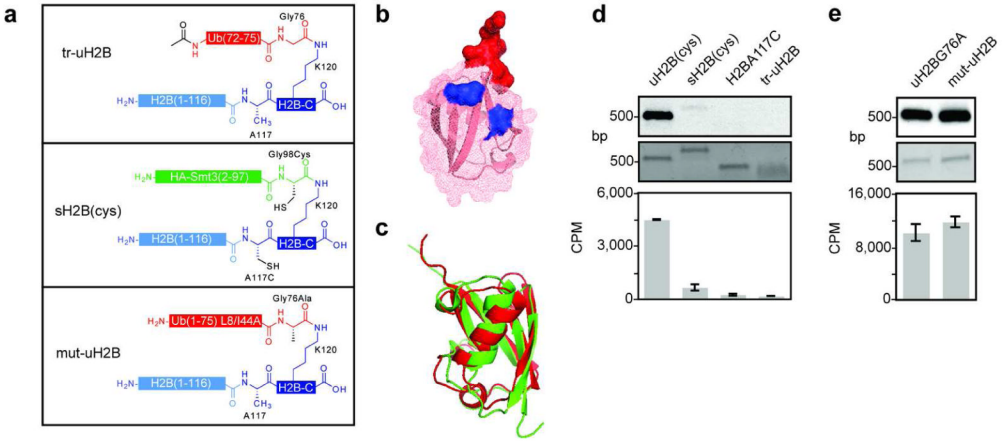

Figure 4. Structure activity relationship analysis of uH2B

a, Schematic of semisynthetic uH2B structural variants. Top panel: H2B bearing the terminal five residues of ubiquitin attached to K120 (tr-uH2B); middle panel: H2B modified with HA-Smt3 with A117C/G98C mutations (sH2B(cys)); bottom panel: uH2BG76A with L8A/I44A double mutation (mut-uH2B). **b,** Ubiquitin structure (1UBQ) (48) represented by superimposed ribbon and mesh diagrams. The surface of the five residues of tr-uH2B are shown in red. Surfaces of L8 and I44 mutated to alanines in mut-uH2B are shown in blue. **c,** Structural alignment of ubiquitin (1UBQ) and Smt3 (1EUV) (37) shown in ribbon diagram. Structures and alignment rendered with PyMol. **d,** Dot1L methyltransferase assay on uH2B structural variants. Nucleosomes containing uH2B(cys), **6**, sH2B(cys), H2B A117C, or tr-uH2B methylated with ^{3}H SAM were separated on native gels and stained with ethidium bromide (middle panel) prior to probing for ^{3}H methyl incorporation by fluorography (top panel). Quantification of methyltransferase activity was performed by filter-binding followed by liquid scintillation counting (bottom panel). **e,** Dot1L assay as in **d**, comparing uH2BG76A and mut-uH2B. Error bars represent one s.d. (n = 3–4).

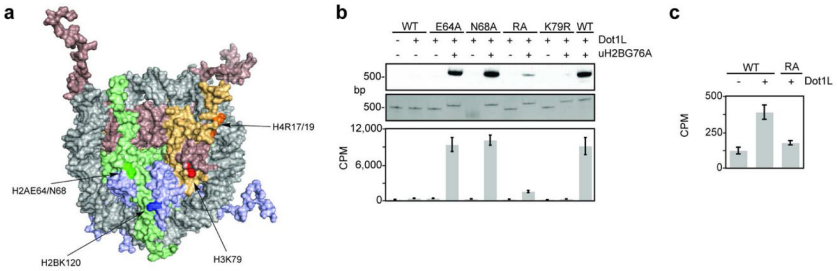

Figure 5. Dot1L assays on mutant nucleosomes

a, Surface representation of nucleosome structure (1KX5) (49) with H2A, H2B, H3, and H4 shown in green, blue, red, and orange, respectively. Amino acids in each histone are emphasized by darker shades. **b,** Dot1L methyltransferase assay on mutant nucleosomes containing H2B or uH2BG76A. Nucleosomes methylated with ^{3}H SAM were separated on native gels and stained with ethidium bromide (middle panel) prior to probing for ^{3}H methyl incorporation by fluorography (top panel). Quantification of methyltransferase activity was performed by filter-binding followed by liquid scintillation counting (bottom panel). Error bars represent one s. d. (n = 3). **c,** Representation of liquid scintillation counting data in **c,** illustrating the effect of the H4R17/19A on Dot1L-mediated methylation of unmodified nucleosomes

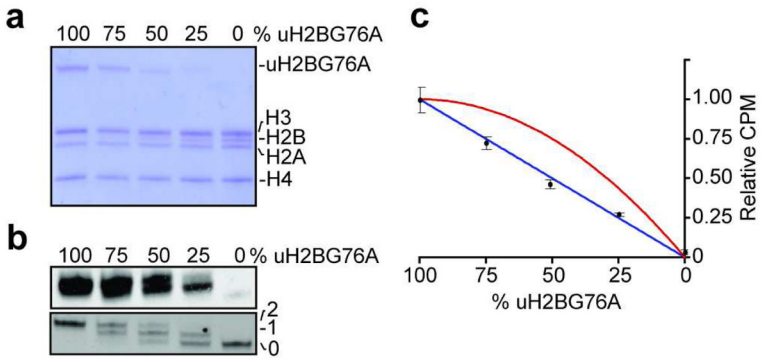

Figure 6. Investigation of ubiquitylation/methylation stoichiometry

a, Octamers formed with varying ratios or uH2BG76A and H2B were separated on a 15% SDS-polyacrylamide gel and stained with Coomassie. **b,** Nucleosomes formed with octamers in **a,** were methylated with Dot1L and ^{3}H SAM. Assay samples were separated by native electrophoresis and stained with ethidium bromide (bottom panel) followed by probing for ^{3}H methyl incorporation by fluorography (top panel). **c,** Quantification of assay samples by filter-binding followed by liquid scintillation counting, plotted relative to the fully ubiquitylated sample. The blue line (rel. CPM = (f_{ub}); where f_{ub} is the fraction of uH2BG76A) represents the case where each uH2BG76A stimulates methylation of only one H3K79 side chain in the same nucleosome. The red line (rel. CPM = $-(f_{ub})^2 + 2(f_{ub})$) represents a case where each uH2BG76A stimulates methylation of both H3K79 side chains in the same nucleosome. Error bars represent one s.d. (n = 4).